

WILLMAN 1 - A GALACTIC SATELLITE AT 40 KPC WITH MULTIPLE STELLAR TAILS

BETH WILLMAN¹, MORAD MASJEDI¹, DAVID W. HOGG¹, JULIANNE J. DALCANTON^{2,3}, DAVID MARTINEZ-DELGADO^{4,5},
MICHAEL BLANTON¹, ANDREW A. WEST^{2,6}, AARON DOTTER⁷, BRIAN CHABOYER⁷

Submitted for publication in AJ

ABSTRACT

SDSSJ1049+5103, commonly known as Willman 1, is an extremely low-luminosity Milky Way companion whose properties are intermediate between those of globular clusters and dwarf spheroidals. In this paper, we present new, wide-field photometry extending 3 mag below the main sequence turnoff. These data show that this object is old, moderately metal-poor, has a distance of 38 ± 7 kpc and a half-light radius of $r_{1/2} = 21 \pm 7$ pc, confirming previous estimates. Willman 1's revised luminosity is $M_V = -2.5$ mag, which is somewhat fainter than the previous estimate. These new data show that the total spatial extent of Willman 1 exceeds its tidal radius for a range of assumptions about its total mass and its orbit, suggesting it is significantly affected by the tidal field of the Milky Way. The spatial distribution of Willman 1's main sequence stars also shows prominent multi-directional stellar tails. The tidal interactions causing these tail features may explain the large physical size of Willman 1 relative to low-luminosity globular clusters. At a distance of 40 kpc, it is the most distant Galactic object yet known to display prominent tails, and is the only distant satellite to display multi-directional tails. Although we cannot at present determine the cause of this unusual morphology, preliminary comparisons between the morphology of Willman 1 and published simulations suggest that it may be near the apocenter of its orbit, or that it may have interacted with another halo object. We find a significant difference between the luminosity functions of stars in the center and in the tails of Willman 1, strongly suggesting mass segregation much like that seen in Palomar 5. Although Willman 1 has more pronounced tidal tails than most confirmed Milky Way dwarf galaxies, because of its very low stellar mass we cannot at present rule out the possibility that it has a dark matter halo.

Subject headings: Galaxy: globular clusters: individual – galaxies: formation — galaxies: dwarfs — Local Group: surveys .

1. INTRODUCTION

The destruction of globular clusters and dwarf galaxies is thought to be an integral part of the formation of the Galactic stellar halo (Searle & Zinn 1978; Ashman & Zepf 1998; Bullock & Johnston 2005). This theory is supported by the observed presence of tidal features around both globular clusters (GCs) and dwarfs. For example, Grillmair et al. (1995) and Leon et al. (2000) found evidence for tidal features in nearly all of the 12 and 20 GCs in their respective samples. The extensively studied tails of Palomar 5 ($d = 23$ kpc) extend over 20 degrees of the sky and contain more stellar mass than the cluster itself (Odenkirchen et al. 2003; Grillmair et al. 2006). More recently, Belokurov et al. (2006) and Grillmair & Johnson (2006) have used SDSS data to trace tails of NGC 5466 ($d = 16$ kpc) over 4 and 45 degrees of sky, respectively.

Like GCs, many of the 10 known Milky Way (MW)

dSphs show signs of tidal stripping. They exhibit breaks in their light profiles that are characteristic of tidal stripping, however the interpretation of both the light and velocity profiles of nearby dwarfs has been controversial (Wilkinson et al. 2004; Munoz et al. 2005). Of these dSphs, only Sagittarius (Sgr; $d = 28$ kpc) exhibits tidal tails as prominent as those seen in globular clusters.

Stellar tails not only provide clues to the formation of the stellar halo, but they also constrain the shape of the MW's dark matter halo and the amount of substructure within it. For example, the Sagittarius tidal stream has been used to measure the shape of the Galactic halo, although there is not yet agreement as to whether the shape is oblate or prolate (Ibata et al. 2001; Helmi 2004; Johnston et al. 2005). The coldness and morphology of tidal tails are affected by the amount of substructure in the Galactic halo, although present comparisons between observations and models of tidal tails have not yet produced strong constraints (Ibata et al. 2002; Johnston et al. 2002; Mayer et al. 2002; Majewski et al. 2004).

Tidal tails can also be used to infer properties intrinsic to the object being stripped. For example, the more a massive Galactic satellite is, the less strongly it is affected by the tidal field of the Milky Way. The presence of tidal features can thus be used to limit the mass-to-light ratios of stripped objects (Oh et al. 1995; Moore 1996; Ibata et al. 1997). The tidal tails of Palomar 5 have provided particularly interesting insights into its past and present properties. Odenkirchen et al. (2003) and Dehnen et al. (2004) used its inferred mass loss rate

¹ New York University, Center for Cosmology and Particle Physics, 4 Washington Place, New York, NY 10003, beth.willman@nyu.edu, david.hogg@nyu.edu mml1330@nyu.edu, mb144@nyu.edu

² Department of Astronomy, University of Washington, Box 351580, Seattle, WA 98195, jd@astro.washington.edu

³ Alfred P. Sloan Research Fellow

⁴ Instituto de Astrofísica de Andalucía (CSIC), Granada, Spain

⁵ Instituto de Astrofísica de Canarias, E-38205 La Laguna, Tenerife, Canary Islands, Spain, ddelgado@iac.es

⁶ Astronomy Department, University of California, Berkeley, CA 94720-3411, awest@astro.berkeley.edu

⁷ Department of Physics & Astronomy, Dartmouth College, Hanover, NH, 03755, aaron.l.dotter@dartmouth.edu, brian.chaboyer@dartmouth.edu

to derive an initial mass that is more than an order of magnitude greater than its present mass. They also used numerical models to determine a life expectancy for Pal 5 of ~ 110 Myr. From the fact that Pal 5's life expectancy is so short, they conclude it is possible that many similar objects once populated the Milky Way's inner halo.

In this paper, we take a detailed look at a low density, outer halo object that we will show shares similarities with Palomar 5. Willman et al. (2005a), hereafter known as Paper I, presented the discovery of SDSSJ1049+5103, an old, moderately metal-poor Milky Way companion. The nature of this object, which is commonly referred to as Willman 1, is ambiguous. In Paper I, we showed that its luminosity and half-light radius place it on the intersection between the size-luminosity relations followed by globular clusters and by old dwarf galaxies. In this paper, we present new wide-field, deep imaging data and make more robust estimates of Willman 1's basic properties. We also show that Willman 1 has prominent multi-directional tails, making it the most distant object observed to have such features. We show it is highly probable that at least some of the tail features are due to tidal interactions with the Milky Way. The purely photometric dataset presented in the paper is still insufficient to either confirm or exclude the possibility that Willman 1 formed inside of its own dark matter halo.

The outline of the paper is as follows. In §2, we describe the observations, data reduction, and completeness tests. In §3 we present results, including the clear presence of stellar tails and evidence for mass segregation of stars. We discuss these results in §4.

2. DATA

We obtained wide-field imaging of Willman 1 with MOSA on the 4m at Kitt Peak National Observatory on 2005 April 7 and 8. This wide-field mosaic camera is composed of $8\ 2048 \times 4096$ chips with $0.26''$ pixels, resulting in a $34' \times 34'$ field of view. Ten 600s exposures were taken through each of the SDSS g and r filters at 5 different positions dithered by ± 30 arcsec and ± 52 arcsec, with seeing varying between $1.2''$ and $1.4''$. Images were bias-subtracted using a sigma-clipped mean of darks (images taken with the shutter closed) and flats were made by taking a sigma-clipped mean of dome flats. The astrometric world coordinate system for each of the eight MOSA chips for each exposure were determined independently by comparison to the USNO-B1.0 astrometric catalog. The DAOPHOT II/ALLSTAR package (Stetson 1994) was used to obtain photometry of the resolved stars. Stellar sources were selected as those identified with $\chi < 2$ and $-0.5 < \text{sharp} < 0.5$ in at least 2 of the 10 exposures in each filter. Stellar magnitudes were photometrically calibrated with the SDSS stellar catalog. The calibration uncertainty varied with exposure and chip number, but is an average of ~ 0.013 magnitudes. The apparent magnitudes were corrected for extinction using the Schlegel et al. (1998) dust maps. The average $E(g-r)$ along the line of sight to Willman 1 is 0.014.

2.1. Completeness Testing

To determine the completeness of the stellar catalog as a function of magnitude, we conducted extensive artificial star tests. We simulated artificial stars with

$22.6 < r < 24.8$ and $0.25 < g - r < 0.65$, the same range as Willman 1's main sequence stars. We inserted a grid of 4500 stars at a time into each exposure of the camera chip that covered Willman 1 and processed the simulated data as described in §2. We repeated this procedure 10 times to simulate a total of 45,000 artificial stars. Artificial stars are considered detected only if: 1) the recovered positions are within $0.5''$ of the input positions, and 2) the recovered magnitude lies within the same 0.5 magnitude bin as the input magnitude. An artificial star coincident with a "real" star is only counted as detected if it is brighter than the real star. With these requirements, we retrieve: $\sim 100\%$ of stars with $r < 22.5$, $\sim 97\%$ of stars with $22.5 < r < 23.0$, $\sim 88\%$ of stars with $23.0 < r < 23.5$, $\sim 84\%$ of stars with $23.5 < r < 24.0$, and $\sim 75\%$ of stars with $24.0 < r < 24.5$. The completeness drops precipitously for stars fainter than 24.5. We thus consider 24.5 to be the completeness limit of our data.

Although the artificial stars have colors and magnitudes consistent with those of Willman 1's main sequence, we have not precisely modeled the expected color-magnitude distribution of stars with the (very uncertain) age, distance and metallicity of Willman 1. This completeness testing is thus not optimized to correct the stellar luminosity function (LF) in an absolute sense, because it does not correctly account for the scattering of stars in and out of the color-magnitude bins used to create the LF in §3.2. However, since this scattering is a second order effect and since our primary concern in §3.5 will be the relative LFs of stars in the outer and inner regions of Willman 1, our estimate of the completeness is sufficient for our scientific goals. Due to the low surface density of Willman 1, crowding does not play a role in the completeness of stars brighter than $r=24.5$. There are only 140 stars brighter than $r=24.5$ within $1.0'$ of Willman 1's center. This translates to a mean spacing of $9''$, which is roughly $7 \times$ the psf. We used our artificial star test to compare the completeness in the field and in the very center ($r < 0.6'$) of Willman 1 and found that they were identical. This comparison confirms that the relative luminosity function presented in §3.5 is accurate.

3. RESULTS

Figure 1 shows the resulting color-magnitude diagram (CMD) of stars within the central $2'$ of Willman 1. This region roughly corresponds to the half-light radius, as derived in Section 3.3. The foreground contamination of this CMD is minimal, so the main sequence of Willman 1 is clearly distinguishable from foreground stars for ~ 3 magnitudes below the turnoff. The mean photometric errors per 0.5 magnitude bin are overplotted. These errors include both measurement and calibration uncertainties. In this Section, we use these color-magnitude data to derive more robust estimates of the properties of Willman 1 than possible with the shallower dataset used in Paper I. We also provide strong evidence that the properties of Willman 1 are affected by tidal forces, and present the first evidence for multi-directional tails and mass segregation.

3.1. Age, metallicity and distance

In Paper I, we compared the colors and magnitudes of the main sequence turnoff (MSTO) and subgiant branch of Willman 1 to those of Palomar 5 and to those of

Girardi et al. (2004) isochrones. We used these comparisons to estimate Willman 1 to be an old, metal-poor population at a distance of 45 ± 10 kpc. We now compare the more precise measurement of Willman 1's MSTO color ($g-r \sim 0.2$) and magnitude ($r \sim 21.9$) to those of the old globular clusters Pal 5, M5, M13, and M15 as observed in SDSS to make a more robust estimate of Willman 1's distance and metallicity. M15 is the most metal-poor of the four comparison clusters, having $[\text{Fe}/\text{H}] \sim -2.3$. The other three have more intermediate metallicities that all fall between -1.2 and -1.6 (Harris 1996). Although M15 has an MSTO color bluer than that of Willman 1, the turnoff color of Willman 1 is consistent with that of the other 3 clusters. This comparison suggests that Willman 1 has $-1.3 \lesssim [\text{Fe}/\text{H}] \lesssim -1.6$. This comparison is somewhat undermined by the fact that turnoff color is sensitive to age as well as metallicity. The red giant branch color 1 - 2 mag brighter than the turnoff is much less sensitive to age than the turnoff color. Pal 5 ($[\text{Fe}/\text{H}] = -1.2$) is the only one of the four clusters with a sub-giant branch that is redder than that of Willman 1, thus providing additional support for our metallicity estimate. Comparing the apparent magnitude of the MSTO of each of the four clusters with that of Willman 1 leads to an average inferred distance of 38 kpc. Assuming the absolute magnitude of Willman 1's MSTO lies in the range of the four comparison clusters, and allowing for an uncertainty in Willman 1's main sequence turnoff of ± 0.1 magnitudes gives a total distance uncertainty of ± 7 kpc.

We also compare the stellar population of Willman 1 to a variety of isochrones to obtain a check of our empirical determination. A finely-spaced grid of old, metal-poor isochrones was constructed with scaled-Solar abundances using an up-to-date version of the Chaboyer et al. (2001) stellar evolution code. Major improvements to the code include the use of low-temperature opacities from Ferguson et al. (2005) and the FreeEOS⁸ equation of state (Irwin 2004). The isochrones were transformed to the observational plane using two methods: first, a purely synthetic method based on PHOENIX model fluxes (Hauschildt et al. 1999a,b) and the throughput curves for SDSS filters⁹; and second, a combination of semi-empirical B and V magnitudes (VandenBerg & Clem 2003) and empirical equations relating B and V to g and r (Smith et al. 2002). Two color transformations were employed to better understand the anticipated shortcomings of each approach. The comparisons of the CMD in Figure 1 with both color transformations support our empirical finding that this object is old (age > 10 Gyr) and metal poor ($[\text{Fe}/\text{H}] \lesssim -1.3$) but without further observational constraints no stronger assertions can be made with an isochrone analysis.

3.2. Absolute Magnitude and Surface Brightness

To improve the estimate of the total luminosity of Willman 1, we compare the luminosity function (LF) of stars within its half-light radius ($r_{1/2} = 1.9'$; see §3.3) with that of Palomar 5. We selected Palomar 5 because it is old, moderately metal-poor, and displays mass segregation like Willman 1 (see §3.1 and 3.5). In addition, its completeness corrected stellar LF is not strongly af-

ected by crowding, and is available in the literature. Koch et al. (2004) presented the B band, foreground and completeness corrected LF of stars within Pal 5's core radius (similar to its half-light radius; Harris 1996). We compute the LF of stars within $r_{1/2}$ of Willman 1 that lie in the main-sequence and sub-giant branch regions of the color magnitude diagram. We then determine the average field star LF in the 960 arcmin² region more distant than $11.4'$ from the center of Willman 1 and subtract it. In Table 1, we summarize these numbers.

To compare the LF to that of Pal 5, we used the transformations of Smith et al. (2002) to convert g and r to B . Within its half-light radius, Pal 5 contains between 7 and $15\times$ the number of stars that Willman 1 contains in each magnitude bin. We only include bins brighter than 2 magnitudes below the MSTO so that completeness does not affect the comparison. We therefore scale the luminosity of Pal 5 by the average LF ratio of 12 to obtain an absolute magnitude of $M_V \sim -2.5$ for Willman 1, consistent with (but a bit fainter than) the preliminary estimate in Paper I. Assuming $M_V = -2.5$ and $r_{1/2} = 1.9'$, the average surface brightness within the half-light radius is 27.7 mag arcsec⁻². We obtain a minimum absolute magnitude of $M_V = -1.4$ by summing the luminosity of the foreground subtracted star counts of stars brighter than $r=24.5$ in the boxed region outlined in Figure 3, assuming a distance of 38 kpc. We thus estimate a generous uncertainty in the M_V of Willman 1 as ± 1 mag.

3.3. Spatial Extent and Tidal Radius

We now use the new data to show that Willman 1 has a half-light radius consistent with that derived in Paper I, but has a larger spatial extent than was possible to determine from the previous data. In Figure 2, we plot the surface density profile of stars that lie within the main sequence color-magnitude box overplotted on the CMD in Figure 1. A mean stellar foreground of 0.44 stars arcmin⁻² (shown by the dotted line) was determined as the average density of stars in the region more than $11.4'$ from the center of Willman 1 that lie in the appropriate color-magnitude box. The resulting profile reaches the foreground level $\sim 10'$ from the object center. Integrating the profile shows that the radius containing half of the stars is $1.9'$. Allowing for an uncertainty of $\pm 0.3'$ in the half-star radius and a distance uncertainty of ± 7 kpc yields a physical size of 21 ± 7 pc, very similar to that derived in Paper I. We assume that this is a reasonable estimate of the half-light radius $r_{1/2}$, since mass segregation (§3.5) affects only the faintest stars, which contribute little to the overall luminosity.

To investigate the possibility that Willman 1 is tidally affected by the Milky Way, we compare its spatial extent to its tidal radius. Figure 2 shows that the total extent of Willman 1 stars is at least $10'$ from its center. We assume it is on a circular orbit, treat the Milky Way as a point mass, and estimate the tidal radius as $r_{\text{tidal}} = R_{\text{sat}}(M_{\text{sat}}/3M_{\text{MW}})^{1/3}$, where R_{sat} is the distance between the satellite and the Milky Way and M_{sat} is the mass of the satellite (Equation 7-84, Binney & Tremaine 1987). We first assume that Willman 1 has a mass of $800 M_{\odot}$. This mass was derived assuming $M_V = -2.5$ (see §3.2) and a mass-to-light ratio of 1, sim-

⁸ Available from <http://freesos.sourceforge.net/>

⁹ <http://www.sdss.org/dr4/instruments/imager/index.html>

TABLE 1
STELLAR LUMINOSITY FUNCTIONS

r	$< r_{half}$		Central		Tail	
	N	N_{corr}	N	N_{corr}	N	N_{corr}
21.50 – 22.0	15.00	14.96	9.00	8.99	17.00	16.85
22.00 – 22.5	16.00	15.71	9.00	8.92	14.00	12.76
22.50 – 23.0	22.00	21.42	10.00	9.84	34.00	31.47
23.00 – 23.5	39.00	37.18	21.00	20.50	48.00	40.02
23.50 – 24.0	27.00	21.15	12.00	10.35	60.00	33.99
24.00 – 24.5	19.00	12.23	6.00	4.12	58.00	28.38

NOTE. — The corrected values only include foreground subtraction; they do not include a completeness correction. The half-light, Central, and Tail areas are 11.34, 3.14, and 49.60 square arcminutes respectively.

ilar to that measured for low luminosity globular clusters by Mandushev et al. (1991). The resulting tidal radius is $r_{tidal} \sim 2'$, comparable to the estimated $r_{1/2}$ and much smaller than the total spatial extent of Willman 1. Although the tidal radius could be much larger if Willman 1 has a substantial dark matter component, an increase in mass by a factor of 10 would still produce a tidal radius significantly smaller than the total extent of its stellar distribution. Furthermore, if Willman 1's orbit is not circular, its tidal radius during parts of its orbit is even smaller than that derived here. It thus is likely that Willman 1 is currently strongly influenced by the tidal field of the Milky Way and is unlikely that Willman 1 is currently in dynamical equilibrium. Palomar 5 is another example of such a stellar system. Dehnen et al. (2004) showed that the azimuthally averaged profile of its central and tail regions suggests its stars extend to 107 pc, while its current tidal radius is only 54 pc currently and was even smaller (by a factor of 2) when Pal 5 was at perihelion.

3.4. Multi-directional Stellar Tails

To further investigate the possibility that Willman 1 is being tidally affected, we constructed a smoothed image of all stars that lie in the main sequence shown on the CMD in Figure 1. Figure 3 shows this image, with contours corresponding to stellar surface densities that are $3 - 20\sigma$ above the field surface density. The image was smoothed with an exponential filter of $0.3'$ scale length. σ was calculated for the distribution of the smoothed surface densities of each image pixel, not including the center of the image. The directions to the Galactic center and to the Ursa Major dwarf galaxy (UMa; only a few degrees away on the sky; Willman et al. 2005b) are overplotted.

The clumpy, tail-like morphology of Willman 1's iso-density contours supports the idea that it is experiencing significant tidal evolution. We obtained shallower observations of Willman 1 on the INT 2.5m in March 2005. Although those observations are less sensitive to the tails at very faint levels, they display the same 3 tail features as the KPNO data. The presence of tails is not surprising, given Willman 1's probable tidal radius. However, such prominent multi-directional features are unusual, particularly for a distant object. Several GCs in the Leon et al. (2000) sample displayed possible multi-directional features, including NGC 288 ($d = 8.1$ kpc). However, of the three most distant GCs in their sample (NGC 5694, 33 kpc; NGC 5824, 32 kpc; NGC 7492, 24.3

kpc), only NGC 5694 and 5824 show strong evidence for tails, and neither show multi-directional tails. Pal 5's ($d = 23$ kpc) extensive tidal tails also do not appear multi-directional.

How did a Milky Way companion at 40 kpc form such an unusual morphology? It is not possible to determine without pursuing additional simulations and obtaining velocity information for this object. However, we infer a couple of possibilities based only on some existing simulations. For example, Figure 6 of Dehnen et al. (2004) shows that a cluster on the derived orbit of Pal 5 is expected to display multi-directional tails when near apogalacticon. The formation of streaky and S-shaped tidal features at apocenter is indeed a natural consequence of tidal tail evolution (Grillmair 1992; C. Grillmair, private communication). Future simulations may thus show that Willman 1's unusual morphology is evidence that it is near the apocenter of its orbit.

Another possibility is that the multiple tails of Willman 1 resulted from gravitational shocking. Disk and bulge shocks are known to play a significant role in the dynamical evolution of globular clusters on orbits that bring them within a few kpc of the Galactic center (Ostriker et al. 1972; Aguilar et al. 1988; Vesperini & Heggie 1997; Gnedin et al. 1999). Combes et al. (1999) showed that multi-directional tails may be observed in objects that have recently experienced gravitational shocking. Such objects display tails perpendicular to the Galactic plane or along the Galactic density gradient. Willman 1's significant distance from the Milky Way makes gravitational shocking from the Milky Way itself an unlikely explanation for the multi-directionality. However, the morphology of Willman 1 could be a combination of the tidal effects of the Milky Way and of interaction with another outer halo object. Knebe et al. (2005) found that satellite-satellite interactions account for $\sim 30\%$ of total satellite mass loss, although penetrating encounters between satellites are relatively rare. Furthermore, preliminary simulations of globular cluster evolution in a Milky Way-like halo have produced clusters with unusual morphologies when the simulated halo includes Cold Dark Matter sub-halos (L. Mayer, private communication). In a future paper, we will pursue a variety of possibilities using numerical simulations informed by velocity data.

3.5. Evidence for Mass Segregation

A relative overabundance of low mass stars has been observed in the outskirts of many Milky Way

globular clusters (King et al. 1995; Lee et al. 2004). There are thought to be two primary sources of this mass segregation in clusters: two-body relaxation (Binney & Tremaine 1987) and a primordial spatial variation of the initial mass function (IMF). Two body interactions transfer energy from more to less massive stars, placing the less massive stars on orbits with higher average radius. Dynamical mass segregation occurs on the relaxation timescale of a system (Binney & Tremaine 1987). However, star clusters that are younger than the relaxation timescale have also been observed to display mass segregation. This is evidence for the existence of primordial mass segregation, whereby the IMF was different at different cluster locations (Bonnell & Davies 1998; Sirianni et al. 2002).

Tidal stripping exacerbates mass segregation because stars that lie at large radii are preferentially stripped. One thus expects that the tidal tails of a mass segregated object will be rich in low mass stars relative to the inner regions of the object. For example, mass segregation has been established in both NGC 288 (Bellazzini et al. 2002) and Palomar 5, low central density clusters that have been shown to be affected by disk shocking. As Koch et al. (2004) explain, unless Palomar 5 used to be much more centrally concentrated it is unlikely that the mass segregation was primarily due to two-body relaxation. Its mass segregation may thus be a combination of primordial and evolutionary effects.

To look for evidence of mass segregation in Willman 1, we compare the stellar luminosity functions of the central and tail regions. In Figure 4, we plot the central and tail LFs plus an arbitrary constant. The error bars include Poisson error in both the number of object stars and in the field subtraction. The “central” region LF includes everything within $1'$ of the object center (area = $3.14'^2$) and the “tail” region includes everything within the boxes outlined on Figure 3 but outside of $1'$ (area = $46.46'^2$). These LFs are summarized in Table 1.

A KS test shows that there is a 68% chance that the two stellar LFs were drawn from different populations. At $\sim 2\sigma$ significance, the central field contains fewer faint, low mass stars than the tail at faint magnitudes. The central LF decreases by 50% in the bin 2 magnitudes fainter than the MSTO ($23.5 < r < 24.0$), whereas the LF of stars in the tail remains nearly constant. This difference between the central and tail LFs cannot be explained by completeness, because our data are not confusion limited (see §2.1). The same is true for stars between $24.0 < r < 24.5$. A similar decrease in the relative number of faint stars in the center and in the tails is also seen in Pal 5. However in Pal 5 the lack of faint stars does not become apparent until 3 magnitudes fainter than its MSTO. In contrast, the lack of faint stars in the center of Willman 1 appears at only 2 magnitudes fainter than the MSTO. This difference suggests that mass segregation may be affecting higher mass stars in Willman 1 than in Pal 5. Deeper imaging will confirm whether this trend continues at fainter magnitudes. We briefly discuss the possible implications of the observed mass segregation in §4.

4. DISCUSSION

In this paper, we have used deep, wide-field imaging to improve estimates of the distance, metallicity, absolute

magnitude, and size of Willman 1. This object has a total luminosity that is similar to that of the least luminous globular clusters. Half-light radius is often used to characterize the size of globular clusters and dwarf galaxies because it does not easily evolve in response to tidal or internal dynamical evolution and is thus a robust reflection of the object’s size at formation. Paper I showed that Willman 1 has a half-light size larger than one might expect for a low luminosity globular cluster, raising the question whether Willman 1 may actually be an extreme dwarf galaxy. In this paper, we have shown evidence that Willman 1 displays: a spatial extent that may exceed its tidal radius, multi-directional tidal tails and possible mass segregation. These results suggest that Willman 1’s large half-light size may be an indication that it is on the verge of disruption rather than an indication that its formation was more similar to that of dwarf galaxies than that of globular clusters.

These new results provide tantalizing hints to the nature of this ambiguous object. The large spatial extent of Willman 1 relative to its tidal radius shows that it is unlikely to be in dynamical equilibrium and that its evolution is being strongly affected by the tidal influence of the Milky Way, even if dark matter makes up 90% of the total mass of the system. As discussed in §3.4, the presence of multiple tidal tails raises several possibilities for the orbit and history of Willman 1. Its multiple tails make Willman 1 a very interesting object to compare with numerical models of substructure evolution in a lumpy galaxy halo, which we will do in a subsequent paper.

The mass segregation observed in Willman 1’s stars has not been previously observed in dwarf galaxies, but rather has only been seen in globular clusters. Although some star clusters provide evidence for primordial mass segregation, most GCs are thought to be mass segregated due to dynamical effects. Because the central stellar densities of known, nearby dwarf galaxies are much lower than those of globular clusters, their relaxation timescales are too long for them to exhibit dynamical mass segregation. Willman 1’s current central density is the same as that of the Milky Way dSphs, but may have been far higher in the past if it has since undergone gravitational shocking. Willman 1 would likely have formed in a similar way to known globular clusters if it had formed with a high enough central density to undergo significant dynamical mass segregation. The situation is less clear if the mass segregation was primordial in origin.

Due to the small stellar mass of Willman 1, these results are still consistent with the possibility suggested by Willman et al. (2005a) that it may have formed within a low mass dark matter halo. Although this scenario is extreme, we discuss it here to underscore the increasingly ambiguous distinction between these two classes of objects (Huxor et al. 2005; Hasegan et al. 2005). The stellar mass of Willman 1 is so small that its spatial extent exceeds its tidal radius even if it is dark matter dominated. Furthermore, it may be difficult for an object as low luminosity as Willman 1 to host multi-directional tails, unless it also hosts a dark matter halo. How long could a $800 M_{\odot}$ object appear to have a coherent structure after experiencing an event that causes prominent multi-directional tails? Preliminary simulations of globular clusters orbiting within a CDM galaxy halo suggest

that very low mass globular clusters are unlikely to remain intact in the event of a substantial tidal event (L. Mayer, private communication). Upcoming multi-object spectroscopy of Willman 1 stars may be able to determine if even its central region is gravitationally bound.

Although the results presented in this paper have shed considerable new light on the nature of Willman 1, the present data still only hint at a range of possibilities for its progenitor. Willman 1's current life expectancy as an object with an order of magnitude fewer stars than Pal 5 may be so short (e.g. few Myr) so as not to expect to ever observe such an object but for a great coincidence. Perhaps many more similar objects used to exist but have been destroyed beyond detection. The extremely small number of stars in Willman 1, and the fact that it contains few, if any, horizontal branch or red giant branch stars exacerbate the difficulty of determining its fundamental properties. Although it contains only a small number of stars bright enough to obtain precise radial velocities for, it is possible that a detailed kinematic study will shed light on Willman 1's mass-to-light ratio and dynamical state. In the future, a combination of

deeper photometry, kinematic data, and numerical modeling will hopefully unravel the mystery of Willman 1.

We acknowledge Carl Grillmair for interesting and informative discussions via email. We thank Anil Seth for discussions that significantly contributed to the stellar photometry and completeness testing. We acknowledge the contributions of Scott Burles, Phil Marshall, and Sam Roweis in the development of the software used to perform the astrometry. MM, DWH, and MRB are partially supported by NASA (LTSA grant NAG5-11669) and the NSF (grant AST-0428465). MM and DWH are grateful to the MIT Kavli Institute for Astrophysics and Space Research for hospitality during the period of this research. JJD. and AAW were partially supported through National Science Foundation grant CAREER AST 02-38683 and the Alfred P. Sloan Foundation. DMD recognizes support by the Spanish Ministry of Education and Science (Ramon y Cajal contract and research project AYA 2001-3939-C03-01)

REFERENCES

- Aguilar, L., Hut, P., & Ostriker, J. P. 1988, *ApJ*, 335, 720
- Ashman, K. M., & Zepf, S. E. 1998, *Globular cluster systems (Globular cluster systems / Keith M. Ashman, Stephen E. Zepf. Cambridge, U. K. ; New York : Cambridge University Press, 1998. (Cambridge astrophysics series ; 30) QB853.5 .A84 1998)*
- Bellazzini, M., Fusi Pecci, F., Montegriffo, P., Messineo, M., Monaco, L., & Rood, R. T. 2002, *AJ*, 123, 2541
- Belokurov, V., Evans, N. W., Irwin, M. J., Hewett, P. C., & Wilkinson, M. I. 2006, *ApJ*, 637, L29
- Binney, J., & Tremaine, S. 1987, *Galactic dynamics* (Princeton, NJ, Princeton University Press, 1987, 747 p.)
- Bonnell, I. A., & Davies, M. B. 1998, *MNRAS*, 295, 691
- Bullock, J. S., & Johnston, K. V. 2005, *astro-ph/0506467*
- Chaboyer, B., Fenton, W. H., Nelan, J. E., Patnaude, D. J., & Simon, F. E. 2001, *ApJ*, 562, 521
- Combes, F., Leon, S., & Meylan, G. 1999, *A&A*, 352, 149
- Dehnen, W., Odenkirchen, M., Grebel, E. K., & Rix, H. 2004, *AJ*, 127, 2753
- Ferguson, J. W., Alexander, D. R., Allard, F., Barman, T., Bodnarik, J. G., Hauschildt, P. H., Heffner-Wong, A., & Tamanai, A. 2005, *ApJ*, 623, 585
- Girardi, L., Grebel, E. K., Odenkirchen, M., & Chiosi, C. 2004, *A&A*, 422, 205
- Gnedin, O. Y., Lee, H. M., & Ostriker, J. P. 1999, *ApJ*, 522, 935
- Grillmair, C. J., & Dionatos, O. 2006, *ApJ* accepted, *astro-ph/0603062*
- Grillmair, C. J. 1992, Ph.D. Thesis
- Grillmair, C. J., Freeman, K. C., Irwin, M., & Quinn, P. J. 1995, *AJ*, 109, 2553
- Grillmair, C. J., & Johnson, R. 2006, *ApJ*, 639, L17
- Haşegan, M. et al. 2005, *ApJ*, 627, 203
- Harris, W. E. 1996, *AJ*, 112, 1487
- Hauschildt, P. H., Allard, F., & Baron, E. 1999a, *ApJ*, 512, 377
- Hauschildt, P. H., Allard, F., Ferguson, J., Baron, E., & Alexander, D. 1999b, *ApJ*, 525, 871
- Helmi, A. 2004, *MNRAS*, 351, 643
- Huxor, A. P., Tanvir, N. R., Irwin, M. J., Ibata, R., Collett, J. L., Ferguson, A. M. N., Bridges, T., & Lewis, G. F. 2005, *MNRAS*, 360, 1007
- Ibata, R., Lewis, G. F., Irwin, M., Totten, E., & Quinn, T. 2001, *ApJ*, 551, 294
- Ibata, R. A., Lewis, G. F., Irwin, M. J., & Quinn, T. 2002, *MNRAS*, 332, 915
- Ibata, R. A., Wyse, R. F. G., Gilmore, G., Irwin, M. J., & Suntzeff, N. B. 1997, *AJ*, 113, 634
- Irwin, A. W. 2004, <http://freeeos.sourceforge.net/documentation.html>
- Johnston, K. V., Law, D. R., & Majewski, S. R. 2005, *ApJ*, 619, 800
- Johnston, K. V., Spergel, D. N., & Haydn, C. 2002, *ApJ*, 570, 656
- King, I. R., Sosin, C., & Cool, A. M. 1995, *ApJ*, 452, L33
- Knebe, A., Power, C., Gill, S. P. D., & Gibson, B. K. 2005, *MNRAS* accepted, *astro-ph/0507380*
- Koch, A., Grebel, E. K., Odenkirchen, M., Martinez-Delgado, D., & Caldwell, J. A. R. 2004, *astro-ph/0408208*
- Lee, K. H., Lee, H. M., Fahlman, G. G., & Sung, H. 2004, *AJ*, 128, 2838
- Leon, S., Meylan, G., & Combes, F. 2000, *A&A*, 359, 907
- Majewski, S. R. et al. 2004, *AJ*, 128, 245
- Mandushev, G., Staneva, A., & Spasova, N. 1991, *A&A*, 252, 94
- Mayer, L., Moore, B., Quinn, T., Governato, F., & Stadel, J. 2002, *MNRAS*, 336, 119
- Moore, B. 1996, *ApJ*, 461, L13
- Munoz, R. R., et al. 2005, *astro-ph/0504035*
- Odenkirchen, M. et al. 2003, *AJ*, 126, 2385
- Oh, K. S., Lin, D. N. C., & Aarseth, S. J. 1995, *ApJ*, 442, 142
- Ostriker, J. P., Spitzer, L. J., & Chevalier, R. A. 1972, *ApJ*, 176, L51+
- Schlegel, D. J., Finkbeiner, D. P., & Davis, M. 1998, *ApJ*, 500, 525
- Searle, L., & Zinn, R. 1978, *ApJ*, 225, 357
- Sirianni, M., Nota, A., De Marchi, G., Leitherer, C., & Clampin, M. 2002, *ApJ*, 579, 275
- Smith, J. A. et al. 2002, *AJ*, 123, 2121
- Stetson, P. B. 1994, *PASP*, 106, 250
- VandenBerg, D. A., & Clem, J. L. 2003, *AJ*, 126, 778
- Vesperini, E., & Heggie, D. C. 1997, *MNRAS*, 289, 898
- Wilkinson, M. I., Kleyana, J. T., Evans, N. W., Gilmore, G. F., Irwin, M. J., & Grebel, E. K. 2004, *ApJ*, 611, L21
- Willman, B. et al. 2005a, *AJ*, 129, 2692
- . 2005b, *ApJ*, 626, L85

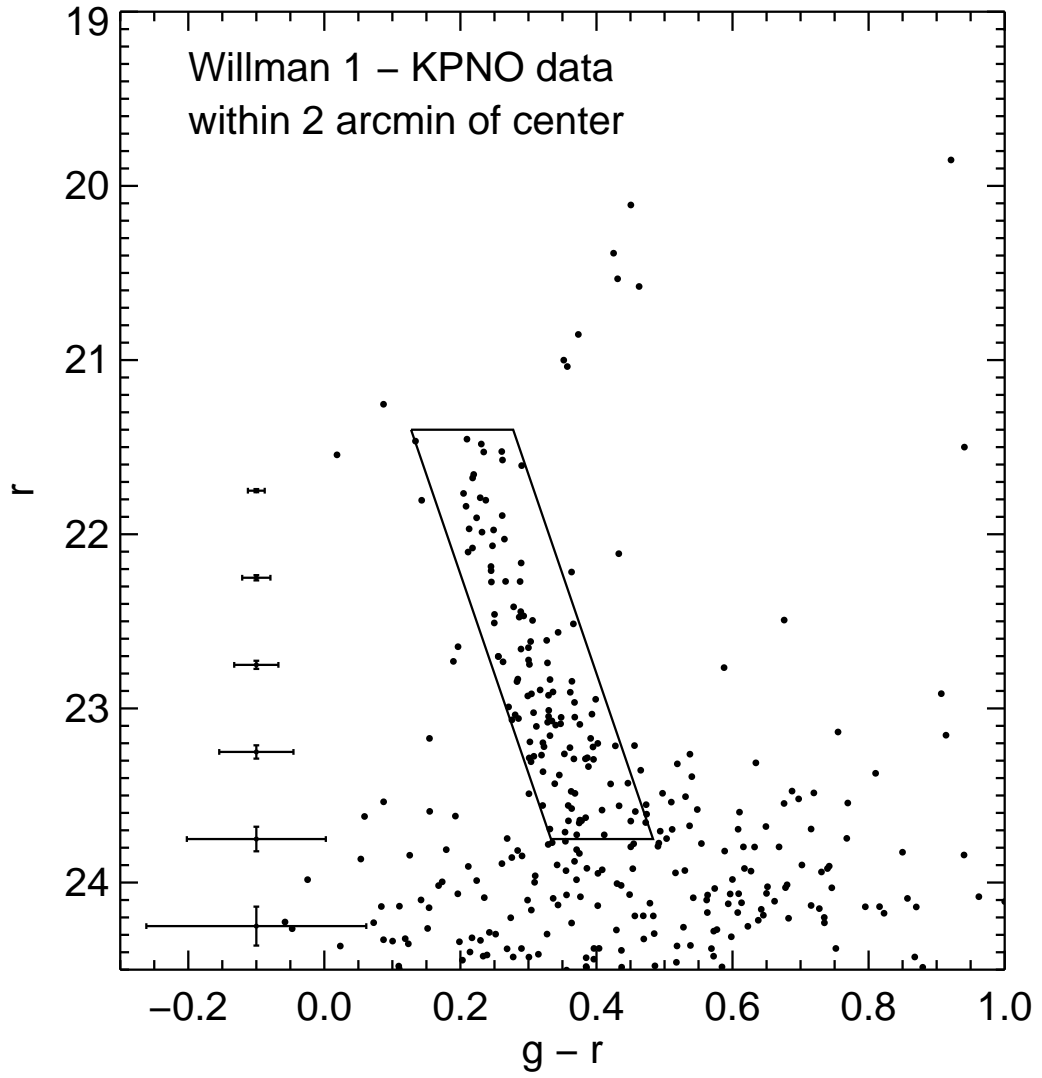


FIG. 1.— The color-magnitude diagram the central 2' of Willman 1. The boxed region shows the color-magnitude range of stars used to produce the stellar density map in Figure 2. A subgiant branch and main sequence are clearly visible in this plot. Average photometric uncertainties including both measurement and calibration errors are overplotted and only include errors of stars within the main-sequence box.

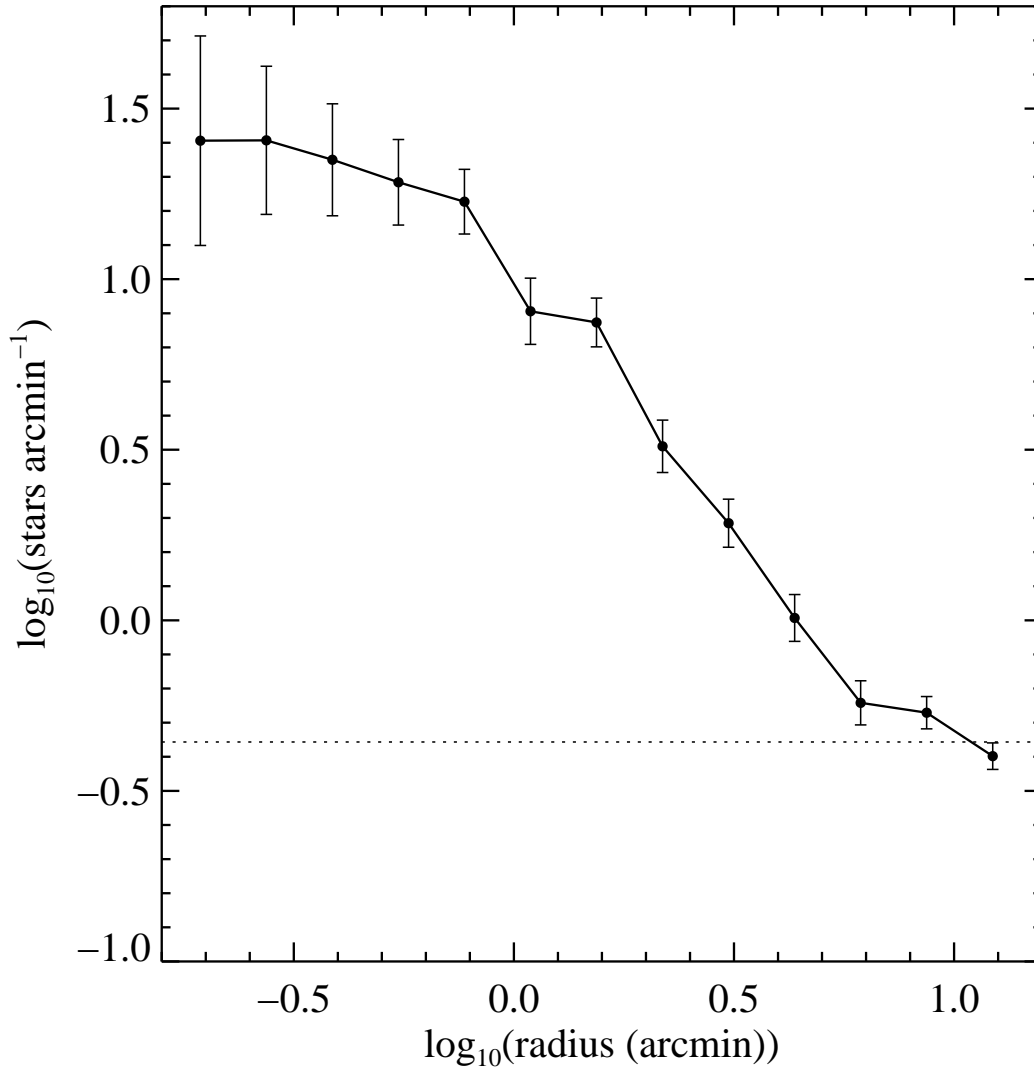


FIG. 2.— The azimuthally averaged radial profile of stars brighter than $r = 23.75$ that lie within the main-sequence box overplotted on Figure 1. The foreground has not been subtracted. The dotted line shows the average number density of main sequence stars more than 5 half-light radii from the center of Willman 1 and brighter than $r = 23.75$. Willman 1 stars extend to at least $10'$ from its center. The error bars were calculated assuming Poisson statistics.

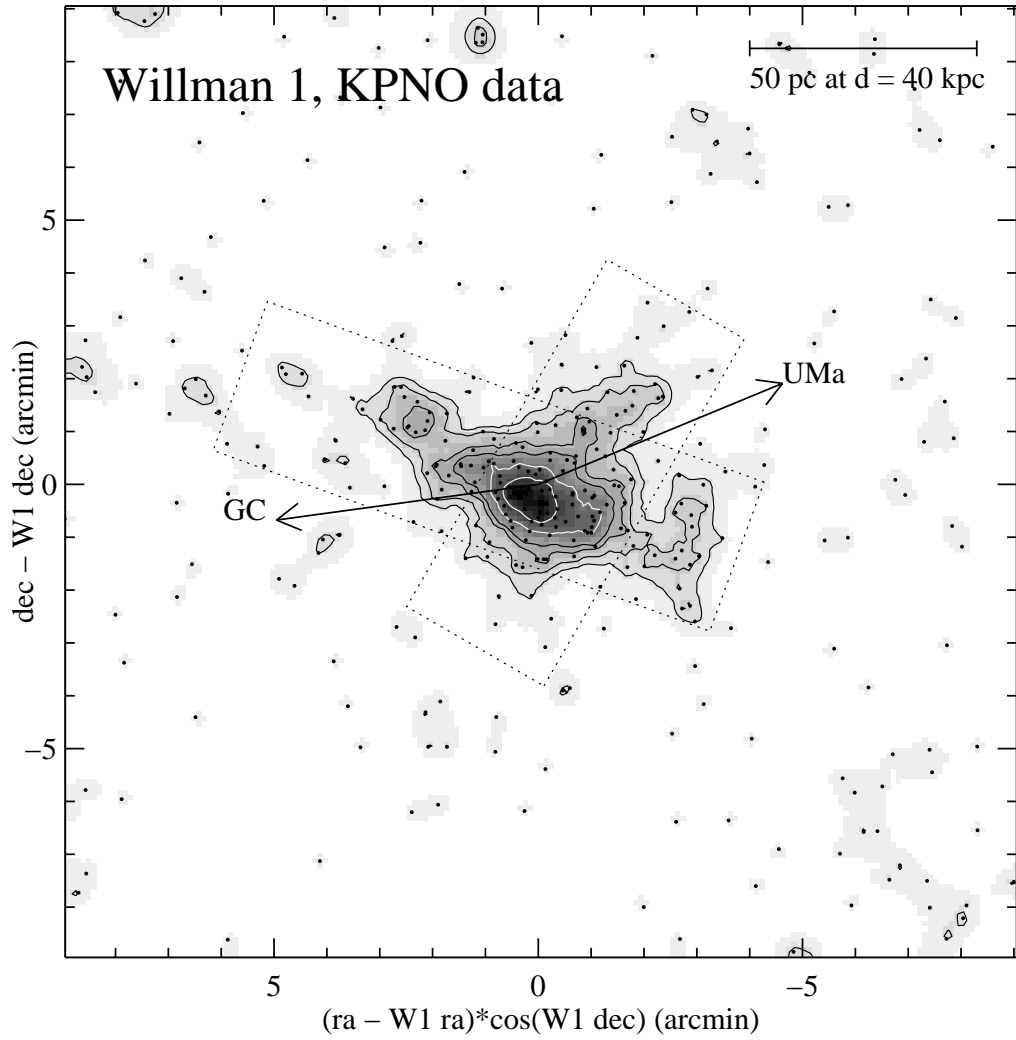


FIG. 3.— Smoothed spatial distribution of stars brighter than $r = 23.75$ that lie within the main-sequence box overlotted on Figure 1. The position of each star used to create this map is shown by a dot in the Figure. The contours correspond to stellar surface densities that are 3, 5, 8, 10, 15, and 20σ above the field surface density. The 15 and 20σ contours are plotted in white. When computing the stellar luminosity function, we define the “tail” as the region outlined by the dotted boxes, but not including the central $1'$. Note the prominent multi-directional tidal features. The directions to the Ursa Major dwarf galaxy and to the Galactic Center are overlotted.

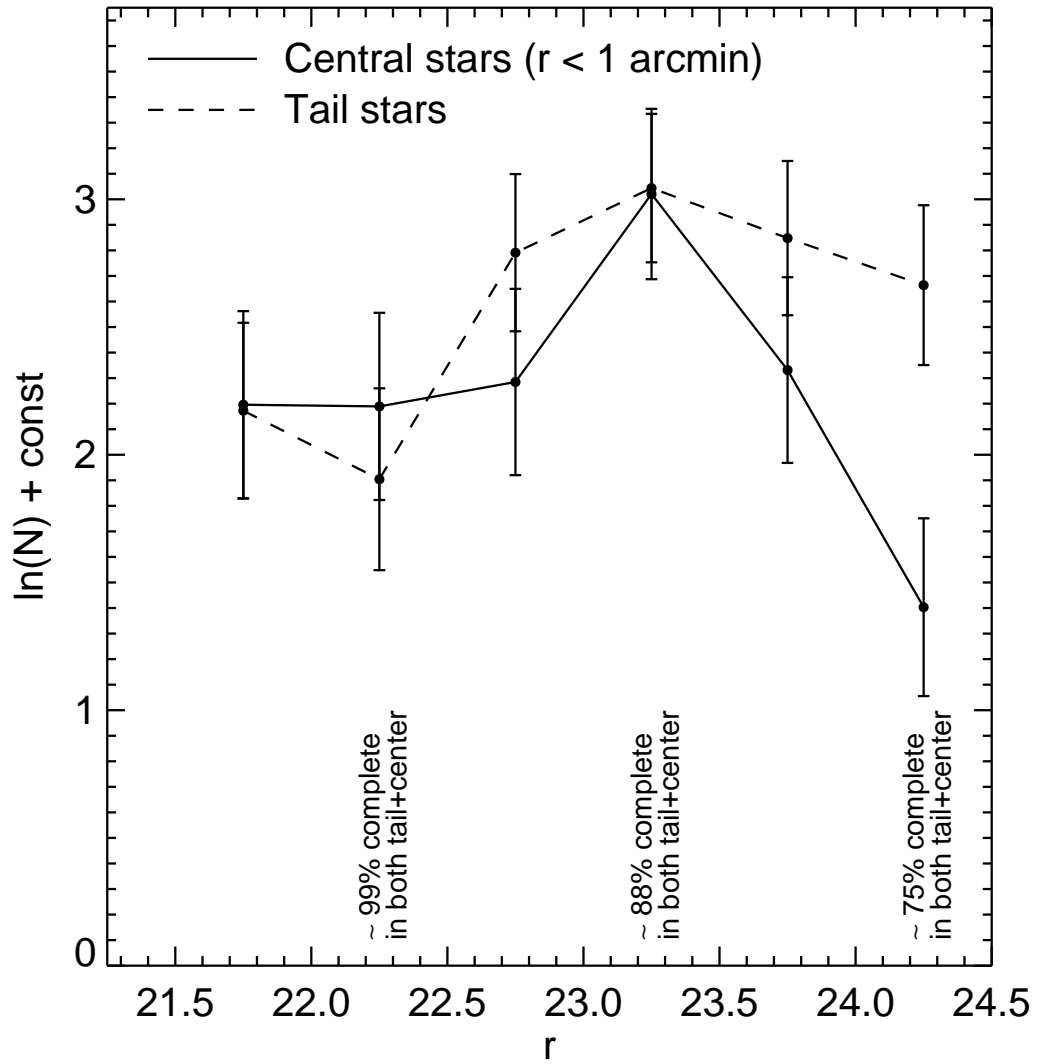


FIG. 4.— The natural log of the foreground corrected luminosity functions of stars within $1'$ of Willman 1 and of stars within the tail regions outlined on Figure 2, but not including stars in the central $1'$. The tail star LF is offset by a constant to facilitate comparison with the central star LF. The bins are 0.5 magnitude wide and bin centers are plotted. The MSTO is near $r = 21.5$. Errors were calculated assuming Poisson fluctuations in the number of object and foreground stars. The tidal tails contain more low luminosity stars than the center at $> 2\sigma$ significance.